*electronics*

MDPI

*Article*

# Demand Response Management via Real-Time Pricing for Microgrid with Electric Vehicles under Cyber-Attack

**Hongbo Zhu [1,2,*], Hui Yin [3], Xue Feng [4], Xinxin Zhang [4] and Zongyao Wang [2,5]**

[1] Faculty of Mathematics and Physics, Huaiyin Institute of Technology, Huai'an 223003, China
[2] Jiangsu Smart Factory Engineering Research Center, Huaiyin Institute of Technology, Huai'an 223003, China
[3] Basic Teaching and Research Department, Shenyang Urban Construction University, Shenyang 110167, China
[4] Department of Mathematics, Aviation University of Air Force, Changchun 130022, China
[5] Faculty of Management Engineering, Huaiyin Institute of Technology, Huai'an 223003, China
* Correspondence: zhb8151@hyit.edu.cn

**Abstract:** The initiative of users to participate in power grid operation is a key factor in realizing the optimal allocation of power. Demand response (DR) management mechanisms based on real-time pricing (RTP) can effectively promote the enthusiasm of users, stimulate the efficiency of microgrids for power dispatch, and achieve the goasl of power peak shifting and valley filling. In this paper, we consider a microgrid composed of several energy providers (EPs) and multiple users, and each user is equipped with several electric vehicles (EVs). It should be noted that EVs may be attacked by networks in the process of data exchange when EVs connect to the MG. In this environment, we establish a multi-time slots social welfare maximization model that reflects the common interests of EPs and users. To simplify the problem, we decompose this multi-time slots model into a set of single-time slot optimization problems by the relaxation method. Furthermore, the mechanisms of identification and processing (MIP) for EVs under cyber-attack are proposed. The problem is decoupled to EPs and users by duality decomposition. Then, through integration with MIP, a distributed RTP algorithm based on the dual subgradient algorithm is designed to obtain the optimal electricity price. Finally, the simulation results verify the feasibility of the model and the effectiveness of the proposed algorithm. Through comparative analysis, the necessity of identifying EVs under cyber-attack is fully embodied.

**Keywords:** demand response; distributed algorithm; electric vehicle; microgrid; real-time pricing

check for updates

**Citation:** Zhu, H.; Yin, H.; Feng, X.; Zhang, X.; Wang, Z. Demand Response Management via Real-Time Pricing for Microgrid with Electric Vehicles under Cyber-Attack. *Electronics* **2023**, *12*, 1321. https://doi.org/10.3390/electronics12061321

Academic Editors: Dmitry Baimel and Inna Katz

Received: 4 February 2023
Revised: 2 March 2023
Accepted: 7 March 2023
Published: 10 March 2023

**Copyright:** © 2023 by the authors. Licensee MDPI, Basel, Switzerland. This article is an open access article distributed under the terms and conditions of the Creative Commons Attribution (CC BY) license (https://creativecommons.org/licenses/by/4.0/).

## 1. Introduction

The rapid development of power electronics technology and the strong support of national environmental protection policies promote the large-scale entry of electric vehicles (EVs) into the market as the main development direction of new energy vehicles. Compared with fuel vehicles, EVs have the advantages of energy saving, environmental protection, good power performance, and low noise [1]. In addition, EVs have charge and discharge characteristics and are good mobile energy storage units. Under the background of a microgrid (MG), the development of vehicle-to-grid (V2G) technology can cut peaks and fill valleys, assist frequency modulation, and reduce system operation costs.

However, due to the uncertainty of EV users' travel rules and charging behavior [2], the distribution of large-scale EV charging load has significant randomness and fluctuations in time and space, which bring certain challenges to the optimal dispatch [3–5], safe operation, planning, and construction of power facilities [6,7]. How to mobilize the enthusiasm of users to cooperate with grid operation, ensure that EVs are connected to the grid in an orderly manner, charge to meet the needs of vehicles during periods of low electricity consumption, and take advantage of the characteristics of energy storage batteries during periods of peak electricity consumption are factors of great significance to the wide application of EVs.

Demand response (DR) is an effective tool for integrating EVs, which can realize synchronous optimization of multiple aspects of coordinated operation and improve the electricity market framework [8–13]. In [14], a two-stage EV automatic DR optimization method based on generalized Glue value-at-risk was put forward to solve existing problems. In order to obtain the ideal cost and profit, a robust method for MG scheduling and optimization of EVs was provided in [15] by Bender decomposition and the Lagrange method. An incentive mechanism based on contract theory was proposed in [16], which customized various contract terms according to the types of EVs to motivate users to participate in DR. The synchronization method based on a complex network proposed in [17] can effectively analyze the dynamic behavior of V2G mobile energy systems. In fact, prices based on DR mechanisms can better mobilize users' enthusiasm and participation in power grid operation. In [18], a charging scheduling problem of EVs based on time-of-use (TOU) price and considering the charging cost constraint was studied and a model was constructed. In [19], through studying the factors involved in the daily operation of the market, an optimal bidding strategy for EV aggregators was proposed. A price-responsive charging scheduling model was proposed in [20], and was beneficial in reducing cost and balancing the load. However, in various optimization strategies for V2G, if users focus on power consumption in the trough period, this causes a rebound effect [21].

Real-time pricing reflects the cost at a moment in the process of power sales, reflecting the characteristic that electricity prices change from moment to moment. This pricing mechanism is an ideal one for power systems [22]. Mohsenian-rad et al. proposed a series of highly innovative RTP models based on pricing principles to maximize social welfare [23–25]. These researches have attracted the attention of relevant scholars and have further improved the model in the past several years. For example, in the models, household appliances were classified [26], wind energy and solar energy were added [27], and power storage devices were considered [28]. In [29], a charging station system based on RTP for vehicle-free and grid-connected EVs was designed to realize the strategy of automatically meeting DR. In [30], an optimal dispatching strategy for aggregators was proposed to maximize their own interests. In these studies, considering the continuity of electric equipment operation, they are analyzed from multiple periods, with time-coupling constraints, but the operation efficiency of the algorithm is restricted.

When EVs are connected to the grid, there is some uncertainty in the process of information exchange. To ensure the safety of electric systems and prevent the occurrence of dangerous accidents, a number of regulations have been formulated. The safety requirements of EV energy supply equipment and those of EV batteries are the two main driving factors. It is still a challenge to quantitatively evaluate the safety of electricity consumption considering the operating conditions of large EV charging stations. Driven by the hazard control mechanism, a comprehensive evaluation method was proposed in [31] to evaluate the safety of large EV charging stations coupled with renewable energy generation. In [32], a DC microgrid network attack detection method and a distributed generator set were proposed. In [33], based on broadcasting many false information messages to the communication network, a self-learn-based attack detection method was proposed, which turned training and prediction into a closed-loop system. In [34], the economic efficiency of the whole system was considered, and the elastic distributed coordination of PEV charging against network attacks was studied, and the detection, isolation, update, and recovery steps were designed comprehensively. Although the above research contribute to a detailed discussion on the safety of V2G systems, they ignore the fact that there is a lack of studies that combine the DR mechanisms to arouse users' enthusiasm.

To make up for the shortcomings of the above research, a MG containing energy providers (EPs), users, attacked EVs, and unattacked EVs is studied in this paper. Table 1 compares the research presented in this paper with current research, and highlights the unique aspects of this paper. A multi-time slots social welfare maximization model reflecting the common interests of EPs and users is built. It studies the mechanisms of identification and processing (MIP) for EVs under cyber-attack and provides a RTP strategy

to further determine the optimal energy scheduling scheme. Therefore, the innovations and contributions of this paper are as follows:

1. Based on the property that a piecewise linear function can approximate any curve, we choose it as the utility function of EVs;
2. Considering EVs under cyber-attack, we build a social welfare maximization model for the whole system;
3. By smoothing the utility function of EVs, the convex optimization method can be used to solve the model. Furthermore, Lagrange multipliers are introduced to transform the multi-time slots' coupling constraint problem into multiple single time slots;
4. The MIP mechanism is proposed to identify EVs under cyber-attack and further deal with them;
5. The RTP algorithm based on the dual subgradient algorithm is designed to coordinate the balance between supply and demand, then the optimal MG energy scheduling strategy is given.

**Table 1.** Summary of some studies on the energy scheduling problems in microgrid.

| References | RTP | Welfare | EV | Multi-EPs | Multi-Time Slots | DR | Cyber Attack |
|---|---|---|---|---|---|---|---|
| [10] | ● | ● | - | - | ● | ● | - |
| [11] | ● | ● | - | ● | - | ● | - |
| [12] | ● | ● | - | - | ● | ● | - |
| [13] | ● | ● | - | ● | ● | ● | - |
| [14] | - | ● | ● | - | ● | ● | - |
| [15] | - | ● | ● | - | - | ● | - |
| [16] | - | - | ● | - | ● | ● | - |
| [29] | ● | - | ● | - | - | ● | - |
| [30] | - | ● | ● | - | ● | - | - |
| [31] | - | - | ● | ● | ● | - | ● |
| [32] | - | - | ● | ● | ● | - | ● |
| [33] | - | - | ● | ● | ● | - | ● |
| [34] | - | - | ● | - | ● | - | ● |
| This article | ● | ● | ● | ● | ● | ● | ● |

● It is mentioned in the article. - It is not mentioned in the article.

The remainder of this paper is organized as follows: The system framework with EPs, users, and EVs is presented in Section 2. In Section 3, we smooth the utility function of EVs; moreover, the Lagrange multipliers are introduced to discretize the model with coupling constraints into a series of single-time slot problems. The dual problem of the constructed model is given in Section 4; at the same time, the MIP considering EVs under cyber-attack is also built. In Section 5, the algorithm combining the RTP information and the dual subgradient algorithm is designed. In Section 6, numerical simulation experiments are carried out to verify the advantages of the model and algorithm through comparative analysis. Section 7 gives the conclusion of the study.

## 2. System Framework

### *2.1. Problem Description*

We introduce a MG with a power scheduling center (PSC), multiple EPs, and many users equipped with several EVs. Every user is equipped with a smart meter. The PSC is a third-party regulator that coordinates the power supply of EPs and demand of users. EPs provide a unified price to users, which can effectively avoid price competition, and they produce the optimal amount of electricity to ensure maximum use and utility. In addition, we consider that there are EVs under cyber-attack. As a result, the information transmitted in the MG system is no longer accurate. Thus, the production and demand of electrical energy do not converge. Therefore, the price is not optimal. So, in each time slot, the users first need to identify and process EVs under cyber-attack.

In order to solve the above problems, we propose a distributed RTP algorithm based on the dual subgradient algorithm (RTP-DSG), which is suitable to obtain the optimal electricity price and the best electricity production.

### *2.2. Utility Function of User*

Normally, we consider a MG comprising $M$ EPs and $N$ users. Every user is equipped with several EVs and a smart meter. The smart meter can control the operation of household appliances, identify cyber-attacked EVs, and formulate the V2G strategy.

We denote the EP set and the user set as $\mathbb{J} = \{1, 2, \cdots, M\}$ and $\mathbb{I} = \{1, 2, \cdots, N\}$, respectively. Suppose one day is a time cycle divided into $K$ time slots; the set is $\mathbb{K} = \{1, 2, \cdots, K\}$. Each user determines how much electricity they use, depending on the price of electricity at different time slots of the day. Denote $x^k_{Load,i}$, $i \in \mathbb{I}$, $k \in \mathbb{K}$, as the power consumption of an essential appliance (except EVs) of user $i$ in time slot $k$. Obviously, there is a certain range of user demand, i.e.,

$$x^{k,\min}_{Load,i} \le x^k_{Load,i} \le x^{k,\max}_{Load,i},\ k \in \mathbb{K}, i \in \mathbb{I}. \tag{1}$$

Here, $x^{k,\min}_{Load,i}$ is the electricity consumption meeting the basic needs of user $i$, and $x^{k,\max}_{Load,i}$ is the power required for all appliances to operate.

The utility function $U^k_{Load,i}(x^k_{Load,i}, \omega^k_{Load,i})$ in microeconomics is used to reflect the satisfaction degree of user $i$ who consumes $x^k_{Load,i}$ energy in time slot $k$. Herein, the elastic coefficient which describes the flexibility of electricity consumption is positive, i.e., $\omega^k_{Load,i} > 0$. In this study, a nondecreasing piecewise function is selected as the utility function [18–21].

$$U^k_{Load,i}(x^k_{Load,i}, \omega^k_{Load,i}) = \begin{cases} \omega^k_{Load,i} x^k_{Load,i} - \frac{\alpha^k_{Load,i}}{2}\left(x^k_{Load,i}\right)^2, & 0 \le x^k_{Load,i} \le \frac{\omega^k_{Load,i}}{\alpha^k_{Load,i}}, \\ \frac{\left(\omega^k_{Load,i}\right)^2}{2\alpha^k_{Load,i}}, & x^k_{Load,i} > \frac{\omega^k_{Load,i}}{\alpha^k_{Load,i}}, \end{cases} \tag{2}$$

where $\alpha^k_{Load,i} > 0$, $i = 1, 2, \cdots, N$ is a given constant.

### *2.3. Cost Function of EP*

Let $y^k_{EP,j}$, $j \in \mathbb{J}$, $k \in \mathbb{K}$, denote the power generation capacity of EP $j$ in time slot $k$. It has upper and lower bounds, denoted by $y^{k,\max}_{EP,j}$ and $y^{k,\min}_{EP,j}$, respectively. So, we have

$$y^{k,\min}_{EP,j} \le y^k_{EP,j} \le y^{k,\max}_{EP,j},\ k \in \mathbb{K}, j \in \mathbb{J}. \tag{3}$$

Generally speaking, according to the actual situation of the energy system, we usually choose the following quadratic function as the cost function for EPs [18–21]:

$$C^k_{EP,j}(y^k_{EP,j}) = a^k_{EP,j}\left(y^k_{EP,j}\right)^2 + b^k_{EP,j} y^k_{EP,j} + c^k_{EP,j},\ k \in \mathbb{K}, j \in \mathbb{J}. \tag{4}$$

where $a^k_{EP,j} > 0$, and $b^k_{EP,j}, c^k_{EP,j} \ge 0$ are predetermined constants.

### *2.4. Electric Vehicle Model*

We assume that each user is equipped with $Q^i_{EV}$ EVs. The EV set of user $i$ is $\mathbb{Q}^i = \left\{1, 2, \cdots, Q^i_{EV}\right\}$. EVs connect to the grid to charge up to a point where the battery capacity is sufficient for the next driving demand. Because the V2G time can be random, EVs have great flexibility, which ensures that they can be arranged to charge, discharge, or idle in the MG at time slot $k$. Let $k^q_{AR,i}, q \in \mathbb{Q}^i$ denote the arrival time of EV $q$, let $k^q_{DE,i}$ denote departure time, and let $\mathbb{K}^q_{EV,i} = \left[k^q_{AR,i}, k^q_{DE,i}\right]$ denote the V2G time. The remaining energy at arrival is $E^q_{AR,i}$ and the target level that is expected to be met or

exceeded is $E^q_{TA,i}$. The total amount of electricity obtained by EV $q$ from the MG at time slot $k$ after arrival is given by

$$E^k_{i,q} = E^q_{AR,i} + \sum_{t=k^q_{AR,i}}^{k} x^{q,t}_{EV,i}, q \in \mathbb{Q}^i, i \in \mathbb{I}, \tag{5}$$

where $x^{q,k}_{EV,i}$ is equal to the charging, discharging, or idle capacity of EV $q$ at time slot $k$.

$$g^q_{DISCH,i} \leq x^{q,k}_{EV,i} \leq g^q_{CH,i}, \ q \in \mathbb{Q}^i, i \in \mathbb{I}. \tag{6}$$

Here, $g^q_{DISCH,i} < 0$ and $g^q_{CH,i} > 0$ are the maximum discharge and charge power, respectively. The primary task of EVs is to meet the driving demand of vehicles, so the battery storage capacity needs to satisfy the following conditions:

$$E^q_{AR,i} + \sum_{k \in \mathbb{K}^q_{EV,i}} x^{q,k}_{EV,i} \geq E^q_{TA,i}, q \in \mathbb{Q}^i, i \in \mathbb{I}. \tag{7}$$

When an EV is not connected to the grid, i.e., $k \notin \mathbb{K}^q_{EV,i}$, the power consumption is zero, so Equation (7) can also be written as Equation (8).

$$E^q_{AR,i} + \sum_{k \in \mathbb{K}} x^{q,k}_{EV,i} \geq E^q_{TA,i}, q \in \mathbb{Q}^i, i \in \mathbb{I}. \tag{8}$$

Normally, the amount of energy stored $E^k_{i,q}$ in EV $q$ needs to be limited to a fixed range in order to prevent over-charging and discharging to ensure battery life, i.e.,

$$E^{\min}_{i,q} \leq E^k_{i,q} \leq E^{\max}_{i,q}. \tag{9}$$

2.4.1. Utility Function of EV

As a piece of special electrical equipment with storage characteristics, EVs can meet users' needs and provide users with a certain satisfaction. In this paper, based on the property that a piecewise linear function can approximate any curve, we choose it as utility function of EV:

$$U^{q,k}_{EV,i}\left(x^{q,k}_{EV,i}, \omega^{q,k}_{EV,i}\right) = \begin{cases} \omega^{q,k}_{1,i} x^{q,k}_{EV,i}, & 0 \leq x^{q,k}_{EV,i} < a^q_{1,i}, \\ \omega^{q,k}_{2,i} x^{q,k}_{EV,i} + (\omega^{q,k}_{1,i} - \omega^{q,k}_{2,i}) a^q_{1,i}, & a^q_{1,i} \leq x^{q,k}_{EV,i} < a^q_{2,i}, \\ \vdots & \vdots \\ \omega^{q,k}_{n,i} x^{q,k}_{EV,i} + (\omega^{q,k}_{1,i} - \omega^{q,k}_{2,i}) a^q_{1,i} + \cdots + (\omega^{q,k}_{n-1,i} - \omega^{q,k}_{n,i}) a^q_{n-1,i}, & a^q_{n-1,i} \leq x^{q,k}_{EV,i} < a^q_{n,i}, \end{cases} \tag{10}$$

where $\omega^{q,k}_{EV,i} = \left[\omega^{q,k}_{1,i}, \omega^{q,k}_{2,i}, \cdots, \omega^{q.k}_{n,i}\right]$ is the elasticity coefficient vector, which describes the enthusiasm of users to connect EVs to the MG. The parameter $\omega^{q,k}_{s,i} (s = 1, 2, \cdots, n)$ is greater than zero, ensuring that the utility function is non-decreasing. Furthermore, the parameter satisfies $\omega^{q,k}_{s,i} \geq \omega^{q,k}_{s+1,i} \geq 0$, which ensures that the marginal utility is decreasing. That is to say, the utility function is a concave function. When $x^{q,k}_{EV,i} < 0$, the EV is discharging; the primary goal of releasing electricity is to supply energy to household appliances, which can reduce the electricity consumption cost for users. Otherwise, when $x^{q,k}_{EV,i} \geq 0$, the EV is charging. To sum up, EV charging can meet driving needs, while discharging can increase utility.

2.4.2. Cost Function of EV

In order to not damage the life of the battery, the energy stored should not fall below the specified threshold, $E_{i,q}^{th} = (1 - DOD_{i,q}^{th})E_{i,q}^{\min}$, where $DOD_{i,q}^{th}$ is the ideal maximum discharge depth of EV $q$. Thus, the energy storage cost at time slot $k$ can be expressed as

$$C_{EV,i}^{q,k} = a_{EV,i}^{q,k} E_{i,q}^{\max} + b_{EV,i}^{q,k}(E_{i,q}^{th} - E_{i,q}^{k}). \tag{11}$$

Here, the first item is investment cost, and the second one is operation cost, which is proportional to the change in EV energy (charge and discharge rate).

*2.5. EVs under Cyber-Attack*

In the context of this study, the data transmission process of EVs may be cyber-attacked. The cyber-attacks mentioned in this paper refer to attacks on the data using loopholes and security defects in the network. If the electricity consumption data exceed the actual data, the EPs provide more electricity and increase the production cost; if the electricity consumption data are lower than the actual data, the actual total electricity production is lower than the total electricity consumption; thus, there is the possibility of power failure. In either case, huge cost losses are caused. Therefore, users must identify and deal with erroneous EV data in a timely manner. We let $\mathbb{Q}_{CA}^{i}$ denote the set of all EVs under cyber-attack. Suppose the electricity consumption data sent by EVs to users are under cyber-attack. In that case, users should identify such EVs and cut off the connection.

On the one hand, this is to avoid the impact on the MG and, on the other hand, reminds users to check their EVs.

The next section describes the mechanism for identifying EVs under cyber-attack during information interactions.

## 3. Problem Formulation

*3.1. Problem Formulation*

In this system, to motivate users to participate in the operation of the MG, we adopted a RTP mechanism. At the beginning of each time slot, the PSC first announces the unit price of electricity, and users determine electricity consumption according to the price to maximize benefits. On the premise that the total supply level of all EPs meets the needs of all users, the objective function is to maximize the total social welfare which is defined as subtracting the total cost of all EPs in the system from the utility of all users. Mathematically, this energy demand process is modeled as the following problem:

(P1)

$$\begin{aligned}\max_{x_{Load,i}^{k}, x_{EV,i}^{q,k}, y_{EP,j}^{k}} & \sum_{k\in\mathbb{K}}\sum_{i\in\mathbb{I}} U_{Load,i}^{k}\left(x_{Load,i}^{k}, \omega_{Load,i}^{k}\right) + \sum_{k\in\mathbb{K}}\sum_{i\in\mathbb{I}}\sum_{q\in\mathbb{Q}^{i}-\mathbb{Q}_{CA}^{i},} U_{EV,i}^{q,k}\left(x_{EV,i}^{q,k}, \omega_{EV,i}^{q,k}\right) \\ & - \sum_{k\in\mathbb{K}}\sum_{j\in\mathbb{J}} C_{EP,j}^{k}\left(y_{EP,j}^{k}\right) - \sum_{k\in\mathbb{K}}\sum_{i\in\mathbb{I}}\sum_{q\in\mathbb{Q}^{i}-\mathbb{Q}^{i}{}_{CA}} C_{EV,i}^{q,k}\left(x_{EV,i}^{q,k}\right)\end{aligned} \tag{12}$$

$$\text{s.t.} \sum_{i\in\mathbb{I}}\left(x_{Load,i}^{k} + \sum_{q\in\mathbb{Q}^{i}-\mathbb{Q}_{CA}^{i}} x_{EV,i}^{q,k}\right) \le \sum_{j\in\mathbb{J}} y_{EP,j}^{k}, \forall k \in \mathbb{K}, \tag{12a}$$

$$E_{AR,i}^{q} + \sum_{k\in\mathbb{K}} x_{EV,i}^{q,k} \ge E_{TA,i}^{q}, q \in \mathbb{Q}^{i} - \mathbb{Q}_{CA}^{i}.i \in \mathbb{I}, \tag{12b}$$

$$E_{i}^{q,\min} \le E_{i}^{q,k} \le E_{i}^{q,\max}, i \in \mathbb{I}, k \in \mathbb{K}, q \in \mathbb{Q}^{i} - \mathbb{Q}_{CA}^{i}, \tag{12c}$$

$$y_{EP,j}^{k,\min} \le y_{EP,j}^{k} \le y_{EP,j}^{k,\max}, j \in \mathbb{J}, k \in \mathbb{K}, \tag{12d}$$

$$x_{Load,i}^{k,\min} \le x_{Load,i}^{k} \le x_{Load,i}^{k,\max}, i \in \mathbb{I}, k \in \mathbb{K}, \tag{12e}$$

$$x_{EV,i}^{q,\min} \le x_{EV,i}^{q,k} \le x_{EV,i}^{q,\max}, i \in \mathbb{I}, k \in \mathbb{K}, q \in \mathbb{Q}^{i} - \mathbb{Q}_{CA}^{i}. \tag{12f}$$

The constraint condition (12a) ensures that the amount of electricity produced by EPs is not less than the total energy consumption in time slot $k$. The constraint (12b) guarantees that EVs meet the driving demand. The remaining restrictions describe the variable range.

### *3.2. Smoothing the Utility Function of EVs*

The utility function $U_{EV,i}^{q,k}(\cdot,\cdot)$ describing the customer satisfaction brought by the operation of EVs is a piecewise linear function. These functions are not differentiable at discontinuities, so the utility function $U_{EV,i}^{q,k}(\cdot,\cdot)$ is not convex. In order to solve this problem and convert it into a convex function, we introduce the smoothing method [35]. A global smooth function $U_{\varepsilon,i}^{q,k}(\cdot,\cdot)$ is constructed to replace the piecewise linear function to ensure that the error is within a very small controllable range.

We first give the general form of the smoothing method. We consider a piecewise linear smooth function with one discontinuity $s$ as follows:

$$f(x) = \begin{cases} m_1 x + n_1, & x \le s, \\ m_2 x + n_2, & x > s. \end{cases} \tag{13}$$

The smooth approximation of this function, on the one hand, should not destroy the properties of other points except the discontinuity point; on the other hand, it should make the function smooth at the discontinuity point. Let us consider the following smooth function:

$$f_\varepsilon(x) = \begin{cases} m_1 x + n_1, & x \le s - \varepsilon, \\ ax^2 + bx + c, & s - \varepsilon < x < s + \varepsilon, \\ m_2 x + n_2, & x \ge s + \varepsilon. \end{cases} \tag{14}$$

Here, the parameters $a$, $b$, and $c$ are parameters to be determined. The following equations should be held:

$$\lim_{x\to(s-\varepsilon)^+} f_\varepsilon(x) = f_\varepsilon(x-\varepsilon),\ \lim_{x\to(s+\varepsilon)^-} f_\varepsilon(x) = f_\varepsilon(x+\varepsilon),\ \lim_{x\to(s-\varepsilon)^+} {f'}_\varepsilon(x) = m_1,\ \lim_{x\to(s+\varepsilon)^-} {f'}_\varepsilon(x) = m_2.$$

Then, we form equations as follows:

$$\begin{cases} a(s-\varepsilon)^2 + b(s-\varepsilon) + c = m_1(s-\varepsilon) + n_1, \\ a(s+\varepsilon)^2 + b(s+\varepsilon) + c = m_2(s+\varepsilon) + n_2, \\ 2a(s-\varepsilon) + b = m_1, \\ 2a(s+\varepsilon) + b = m_2. \end{cases} \tag{15}$$

By solving the equations, we obtain

$$a = \frac{m_2 - m_1}{4\varepsilon},\ b = \frac{m_1 + m_2}{2} - \frac{(m_2 - m_1)s}{2\varepsilon},\ c = \frac{(s^2 + \varepsilon^2)(m_1 - m_2)}{4\varepsilon} + \frac{n_1 + n_2}{2}. \tag{16}$$

In this way, the smooth approximation function $f_\varepsilon(x)$ of function $f(x)$ is obtained. The approximation degree of function $f_\varepsilon(x)$ to $f(x)$ increases with a decrease in $\varepsilon$, i.e., when $\varepsilon \to 0^+$, $f_\varepsilon(x) \to f(x)$.

According to the above method, each discontinuity point of the piecewise linear function can be smoothed, and a smooth function $U_{\varepsilon,i}^{q,k}(\cdot,\cdot)$ is obtained to replace function $U_{EV,i}^{q,k}(\cdot,\cdot)$ approximately. Then, question P1 is transformed into P2 in the following form:

(P2)

$$\begin{aligned} \max_{x_{Load,i}^k, x_{EV,i}^{q,k}, y_{EP,j}^k} & \sum_{k\in\mathbb{K}}\sum_{i\in\mathbb{I}} U_{Load,i}^k\left(x_{Load,i}^k, \omega_{Load,i}^k\right) + \sum_{k\in\mathbb{K}}\sum_{i\in\mathbb{I}}\sum_{q\in\mathbb{Q}^i-\mathbb{Q}_{CA}^i} U_{\varepsilon,i}^{q,k}\left(x_{EV,i}^{q,k}, \omega_{EV,i}^{q,k}\right) \\ & - \sum_{k\in\mathbb{K}}\sum_{j\in\mathbb{J}} C_{EP,j}^k\left(y_{EP,j}^k\right) - \sum_{k\in\mathbb{K}}\sum_{i\in\mathbb{I}}\sum_{q\in\mathbb{Q}^i-\mathbb{Q}_{CA}^i} C_{EV,i}^{q,k}\left(x_{EV,i}^{q,k}\right) \end{aligned} \tag{17}$$

s.t. (12a)–(12f)

By definition, utility functions $U^k_{Load,i}(\cdot,\cdot)$ and $U^{q,k}_{\varepsilon,i}(\cdot,\cdot)$ are strictly concave and cost functions $C^k_{EP,j}(\cdot)$ and $C^{q,k}_{EV,i}(\cdot)$ are strictly convex when $k \in \mathbb{K}$, $i \in \mathbb{I}$. By virtue of the operation properties of convex functions, it can be concluded that the objective function (17) is strictly concave. In addition, the constraint conditions of P2 are affine, and the constraint set is a nonempty closed convex set. In summary, problem P2 is a strictly convex programming problem. Therefore, problem P2 has a unique global optimum [36].

### *3.3. Temporally Coupled Constraint and Relaxation*

The constraints (12b) and (12c) are actually time-coupled constraints that couple together all time slots of a day. Such constraints make it challenging to solve P2 individually at each time slot. Therefore, we relax the constraints (12b) and (12c) by introducing Lagrange multipliers $v^q_{EV,i} \geq 0$, and $\theta^q_{EV,i} \geq 0$ for each user as

$$
\begin{aligned}
&\max_{x^k_{Load,i},x^{q,k}_{EV,i},y^k_{EP,j}} \sum_{k\in\mathbb{K}}\sum_{i\in\mathbb{I}} U^k_{Load,i}\left(x^k_{Load,i},\omega^k_{Load,i}\right)+\sum_{k\in\mathbb{K}}\sum_{i\in\mathbb{I}}\sum_{q\in\mathbb{Q}^i-\mathbb{Q}^i_{CA}} U^{q,k}_{\varepsilon,i}\left(x^{q,k}_{EV,i},\omega^{q,k}_{EV,i}\right)\\
&\quad-\sum_{k\in\mathbb{K}}\sum_{j\in\mathbb{J}} C^k_{EP,j}\left(y^k_{EP,j}\right)-\sum_{k\in\mathbb{K}}\sum_{i\in\mathbb{I}}\sum_{q\in\mathbb{Q}^i-\mathbb{Q}^i_{CA}} C^{q,k}_{EV,i}\left(x^{q,k}_{EV,i}\right)-\sum_{i\in\mathbb{I}}\sum_{q\in\mathbb{Q}^i-\mathbb{Q}^i_{CA}} v^q_{EV,i}\left(E^q_{AR,i}+\sum_{k\in\mathbb{K}} x^{q,k}_{EV,i}-E^q_{TA,i}\right)\\
&\quad+\sum_{i\in\mathbb{I}}\sum_{q\in\mathbb{Q}^i-\mathbb{Q}^i_{CA}} \theta^q_{EV,i}\left(E^q_{AR,i}+\sum_{k\in\mathbb{K}} x^{q,k}_{EV,i}-E^{\max}_{i,q}\right)\\
&=\max_{x^k_{Load,i},x^{q,k}_{EV,i},y^k_{EP,j}} \sum_{k\in\mathbb{K}}\Bigg[\sum_{i\in\mathbb{I}} U^k_{Load,i}\left(x^k_{Load,i},\omega^k_{Load,i}\right)+\sum_{i\in\mathbb{I}}\sum_{q\in\mathbb{Q}^i-\mathbb{Q}^i_{CA}} U^{q,k}_{\varepsilon,i}\left(x^{q,k}_{EV,i},\omega^{q,k}_{EV,i}\right)\\
&\quad-\sum_{j\in\mathbb{J}} C^k_{EP,j}\left(y^k_{EP,j}\right)-\sum_{i\in\mathbb{I}}\sum_{q\in\mathbb{Q}^i-\mathbb{Q}^i_{CA}} C^{q,k}_{EV,i}\left(x^{q,k}_{EV,i}\right)-\sum_{i\in\mathbb{I}}\sum_{q\in\mathbb{Q}^i-\mathbb{Q}^i_{CA}} (v^q_{EV,i}-\theta^q_{EV,i})x^{q,k}_{EV,i}\Bigg]\\
&\quad-\sum_{i\in\mathbb{I}}\sum_{q\in\mathbb{Q}^i-\mathbb{Q}^i_{CA}}\left[v^q_{EV,i}\left(E^q_{AR,i}-E^q_{TA,i}\right)-\theta^q_{EV,i}\left(E^q_{AR,i}-E^{\max}_{i,q}\right)\right]\\
&=\max_{x^k_{Load,i},x^{q,k}_{EV,i},y^k_{EP,j}} \sum_{k\in\mathbb{K}}\Bigg\{\sum_{i\in\mathbb{I}}\Bigg[U^k_{Load,i}\left(x^k_{Load,i},\omega^k_{Load,i}\right)+\sum_{q\in\mathbb{Q}^i-\mathbb{Q}^i_{CA}} U^{q,k}_{\varepsilon,i}\left(x^{q,k}_{EV,i},\omega^{q,k}_{EV,i}\right)\\
&\quad-\sum_{q\in\mathbb{Q}^i-\mathbb{Q}^i_{CA}} C^{q,k}_{EV,i}\left(x^{q,k}_{EV,i}\right)-\sum_{q\in\mathbb{Q}^i-\mathbb{Q}^i_{CA}} (v^q_{EV,i}-\theta^q_{EV,i})x^{q,k}_{EV,i}\Bigg]-\sum_{j\in\mathbb{J}} C^k_{EP,j}\left(y^k_{EP,j}\right)\Bigg\}\\
&\quad-\sum_{i\in\mathbb{I}}\sum_{q\in\mathbb{Q}^i-\mathbb{Q}^i_{CA}}\left[v^q_{EV,i}\left(E^q_{AR,i}-E^q_{TA,i}\right)-\theta^q_{EV,i}\left(E^q_{AR,i}-E^{\max}_{i,q}\right)\right].
\end{aligned}
\tag{18}
$$

The Lagrange multiplier $v^q_{EV,i}$ corresponding to the constraints of driving needs can be iteratively solved by

$$
v^{q,t+1}_{EV,i}=\left[v^{q,t}_{EV,i}-d_1\left(E^q_{AR.i}+\sum_{k\in\mathbb{K}}\widetilde{x}^{q,t}_{EV,i}-E^q_{TA,i}\right)\right]^+, \tag{19}
$$

where $[\cdot]$ denotes $\max\{\cdot,0\}$, the plus function. The step size $d_1$ can adjust the convergence rate, $t \in \mathbb{N}^+$ represents the number of iterations, and $\widetilde{x}^{q,t}_{EV,i}$ is the solution to Equation (8) for a given $v^{q,t}_{EV,i}$.

If the driving demand is satisfied, the charging of EVs must be greater than the lower limit. We only need to consider the upper-limit constraint of EV charging. The Lagrange multiplier $\theta^q_{EV,i}$ corresponding to an upper limit of EV charging can be iteratively solved by

$$
\theta^{q,t+1}_{EV,i}=\left[\theta^{q,t}_{EV,i}+d_2\left(E^q_{AR.i}+\sum_{k\in\mathbb{K}}\widetilde{x}^{q,t}_{EV,i}-E^{\max}_{i,q}\right)\right]^+. \tag{20}
$$

Here, parameter $d_2$ is the step size, and $v^q_{EV,i}$ and $\theta^q_{EV,i}$ are updated by user $i$ without notice to any other user. Therefore, the original problem P2, which considers the whole time cycle, is transformed into each time slot for optimization [37], that is, problem P2 is transformed into equivalent one, P3:

(P3)

$$\begin{aligned}\max_{\substack{X^k_{Load}\in\mathbb{X}^k_{Load}\\ X^k_{EV}\in\mathbb{X}^k_{EV}\\ y^k_{EP}\in\mathbb{Y}^k_{EP}}} \sum_{i\in\mathbb{I}}\Bigg[U^k_{Load,i}\left(x^k_{Load,i},\omega^k_{Load,i}\right)+\sum_{q\in\mathbb{Q}^i-\mathbb{Q}^i_{CA}}U^{q,k}_{\varepsilon,i}\left(x^{q,k}_{EV,i},\omega^{q,k}_{EV,i}\right)\\ -\sum_{q\in\mathbb{Q}^i-\mathbb{Q}^i_{CA}}C^{q,k}_{EV,i}\left(x^{q,k}_{EV,i}\right)-\sum_{q\in\mathbb{Q}^i-\mathbb{Q}^i_{CA}}\left(v^q_{EV,i}-\theta^q_{EV,i}\right)x^{q,k}_{EV,i}\Bigg]-\sum_{j\in\mathbb{J}}C^k_{EP,j}\left(y^k_{EP,j}\right)\end{aligned} \tag{21}$$

$$\text{s.t.}\sum_{i\in\mathbb{I}}\left(x^k_{Load,i}+\sum_{q\in\mathbb{Q}^i-\mathbb{Q}^i_{CA}}x^{q,k}_{EV,i}\right)\le\sum_{j\in\mathbb{J}}y^k_{EP,j}. \tag{21a}$$

## 4. Dual Problem and the MIP

### *4.1. Dual Problem*

We propose a distributed dual subgradient optimization algorithm, which conveniently solves the problem P3 and greatly improves the information exchange rate.

The Lagrange function related to P3 is:

$$\begin{aligned}\mathcal{L}\left(X^k_{Load},X^k_{EV},Y^k_{EP},\lambda^k\right)&=\sum_{i\in\mathbb{I}}\Bigg[U^k_{Load,i}\left(x^k_{Load,i},\omega^k_{Load,i}\right)+\sum_{q\in\mathbb{Q}^i-\mathbb{Q}^i_{CA}}U^{q,k}_{\varepsilon,i}\left(x^{q,k}_{EV,i},\omega^{q,k}_{EV,i}\right)\\ &\quad-\sum_{q\in\mathbb{Q}^i-\mathbb{Q}^i_{CA}}C^{q,k}_{EV,i}\left(x^{q,k}_{EV,i}\right)-\sum_{q\in\mathbb{Q}^i-\mathbb{Q}^i_{CA}}\left(v^q_{EV,i}-\theta^q_{EV,i}\right)x^{q,k}_{EV,i}\Bigg]-\sum_{j\in\mathbb{J}}C^k_{EP,j}\left(y^k_{EP,j}\right)\\ &\quad-\lambda^k\left[\sum_{i\in\mathbb{I}}\left(x^k_{Load,i}+\sum_{q\in\mathbb{Q}^i-\mathbb{Q}^i_{CA}}x^{q,k}_{EV,i}\right)-\sum_{j\in\mathbb{J}}y^k_{EP,j}\right]\\ &=\sum_{i\in\mathbb{I}}\Bigg[U^k_{Load,i}\left(x^k_{Load,i},\omega^k_{Load,i}\right)+\sum_{q\in\mathbb{Q}^i-\mathbb{Q}^i_{CA}}U^{q,k}_{\varepsilon,i}\left(x^{q,k}_{EV,i},\omega^{q,k}_{EV,i}\right)\\ &\quad-\sum_{q\in\mathbb{Q}^i-\mathbb{Q}^i_{CA}}C^{q,k}_{EV,i}\left(x^{q,k}_{EV,i}\right)-\sum_{q\in\mathbb{Q}^i-\mathbb{Q}^i_{CA}}\left(v^q_{EV,i}-\theta^q_{EV,i}\right)x^{q,k}_{EV,i}-\lambda^k\left(x^k_{Load,i}+\sum_{q\in\mathbb{Q}^i-\mathbb{Q}^i_{CA}}x^{q,k}_{EV,i}\right)\Bigg]\\ &\quad+\sum_{j\in\mathbb{J}}\left[\lambda^k y^k_{EP,j}-C^k_{EP,j}\left(y^k_{EP,j}\right)\right].\end{aligned} \tag{22}$$

The Lagrange multiplier $\lambda^k\ge 0$, associated with global inequality constraints, is usually used to indicate electricity price.

Mathematically, the Lagrange function is as follows:

$$D(\lambda^k)=\max_{X^k_{Load},X^k_{EV},Y^k_{EP}}\mathcal{L}(X^k_{Load},X^k_{EV},Y^k_{EP},\lambda^k)=\sum_{i\in\mathbb{I}}S^k_i(\lambda^k)+\sum_{j\in\mathbb{J}}T^k_j(\lambda^k),$$

where $\lambda^k\ge 0,\ k\in\mathbb{K}$, and

$$
\begin{aligned}
S_i^k(\lambda^k) &= \max_{X_{Load}^k, X_{EV}^k} \Bigg[ U_{Load,i}^k\left(x_{Load,i}^k, \omega_{Load,i}^k\right) + \sum_{q\in\mathbb{Q}^i-\mathbb{Q}_{CA}^i} U_{\varepsilon,i}^{q,k}\left(x_{EV,i}^{q,k}, \omega_{EV,i}^{q,k}\right) \\
&\quad - \sum_{q\in\mathbb{Q}^i-\mathbb{Q}_{CA}^i} C_{EV,i}^{q,k}\left(x_{EV,i}^{q,k}\right) - \sum_{q\in\mathbb{Q}^i-\mathbb{Q}_{CA}^i}\left(v_{EV,i}^q - \theta_{EV,i}^q\right)x_{EV,i}^{q,k} - \lambda^k\left(x_{Load,i}^k + \sum_{q\in\mathbb{Q}^i-\mathbb{Q}_{CA}^i} x_{EV,i}^{q,k}\right)\Bigg] \\
&= S_{i,1}^k(\lambda^k) + S_{i,2}^k(\lambda^k),
\end{aligned}
$$

$$
S_{i,1}^k(\lambda^k) = \max_{X_{Load}^k}\left[U_{Load,i}^k\left(x_{Load,i}^k, \omega_{Load,i}^k\right) - \lambda^k x_{Load,i}^k\right], \tag{23}
$$

$$
S_{i,2}^k(\lambda^k) = \max_{X_{EV}^k} \sum_{q\in\mathbb{Q}^i-\mathbb{Q}_{CA}^i}\left[U_{\varepsilon,i}^{q,k}\left(x_{EV,i}^{q,k}, \omega_{EV,i}^{q,k}\right) - C_{EV,i}^{q,k}\left(x_{EV,i}^{q,k}\right) - \left(v_{EV,i}^q - \theta_{EV,i}^q\right)x_{EV,i}^{q,k} - \lambda^k x_{EV,i}^{q,k}\right], \tag{24}
$$

$$
T_j^k(\lambda^k) = \max_{Y_{EP}^k}\left[\lambda^k y_{EP,j}^k - C_{EP,j}^k\left(y_{EP,j}^k\right)\right]. \tag{25}
$$

The dual problem is as follows:

$$
\min_{\lambda^k\geq 0} D(\lambda^k). \tag{26}
$$

The gradient projection method is introduced to solve the dual optimization problem iteratively, and the PSC updates the price $\lambda_t^k$ according to the following formula:

$$
\lambda_{t+1}^k = \left[\lambda_t^k + d_3\left(\sum_{i\in\mathbb{I}}\left(x_{Load,i}^k + \sum_{q\in\mathbb{Q}^i-\mathbb{Q}_{CA}^i} x_{EV,i}^{q,k}\right) - \sum_{j\in\mathbb{J}} y_{EP,j}^k\right)\right]^+, \tag{27}
$$

where $d_3$ is the iteration step size. Problem P3 can be transformed into solving for EPs, users, and EVs three types of subproblems (23)–(25) due to the separable nature of the dual problem (26).

### *4.2. Identifying and Processing EVs under Cyber-Attack*

Considering that the utility function of EVs is described by a piecewise function (10), we consider a segmentation point, and the others are similar. Near the segmentation point $a_1$ and with the aid of Equation (16), we have

$$
U_{\varepsilon,i}^{q,k} = \begin{cases} \omega_{1,i}^{q,k} x_{EV,i}^{q,k}, & 0 \leq x_{EV,i}^{q,k} \leq a_1 - \varepsilon, \\ a_{EV,1}^{q,k}\left(x_{EV,i}^{q,k}\right)^2 + b_{EV,1}^{q,k} x_{EV,i}^{q,k} + c_{EV,1}^{q,k}, & a_1 - \varepsilon \leq x_{EV,i}^{q,k} \leq a_1 + \varepsilon, \\ \omega_{2,i}^{q,k} x_{EV,i}^{q,k} + \left(\omega_{1,i}^{q,k} - \omega_{2,i}^{q,k}\right)a_1, & a_1 + \varepsilon \leq x_{EV,i}^{q,k} \leq a_2 - \varepsilon, \end{cases} \tag{28}
$$

where $a_{EV,1}^{q,k} = \frac{\omega_{1,i}^{q,k} - \omega_{2,i}^{q,k}}{4\varepsilon}$, $b_{EV,1}^{q,k} = \frac{\omega_{1,i}^{q,k} + \omega_{2,i}^{q,k}}{2} - \frac{a_1(\omega_{1,i}^{q,k} - \omega_{2,i}^{q,k})}{2\varepsilon}$ and

$$
c_{EV,1}^{q,k} = \frac{({a_1}^2 + \varepsilon^2)(\omega_{1,i}^{q,k} - \omega_{2,i}^{q,k})}{4\varepsilon} + \frac{a_1(\omega_{1,i}^{q,k} - \omega_{2,i}^{q,k})}{2}.
$$

Furthermore, according to Equations (24) and (28), we obtain

$$
x_{EV,i}^{q,k*}(\lambda_t^k) = \underset{q\in\mathbb{Q}^i-\mathbb{Q}_{CA}^i}{\operatorname{argmax}}\left[U_{\varepsilon,i}^{q,k}(x_{EV,i}^{q,k}, \omega_{EV,i}^{q,k}) - C_{EV,i}^{q,k}\left(x_{EV,i}^{q,k}\right) - \left(v_{EV,i}^q - \theta_{EV,i}^q\right)x_{EV,i}^{q,k} - \lambda^k x_{EV,i}^{q,k}\right]. \tag{29}
$$

In this paper, the parameter $\omega_{EV,i}^{q,k} = \left[\omega_{1,i}^{q,k}, \omega_{2,i}^{q,k}, \cdots, \omega_{n,i}^{q,k}\right]$ involves $n$ different constants at time slot $k$ of user $i$. In time slot $k$, if PSC has received $n$ different values of optimal power demand in the $t$th iteration to the $(t+n-1)$th one, denoted by $x_{EV,i}^{q,k*}(\lambda_t^k)$

to $x_{EV,i}^{q,k*}(\lambda_{t+n-1}^{k})$, respectively. Next, we determine whether $x_{EV,i}^{q,k*}(\lambda_{r}^{k})$, $r = t, t+1, \cdots, t+n-1$, is equal to $x_{EV,i}^{q,\min}$ or $x_{EV,i}^{q,\max}$. If neither is true, then user $i$ needs to solve the following Equation (30) and obtain the parameters $\omega_{EV,i}^{q,k}$ of EV $q$ in time slot $k$.

$$\left[U_{\varepsilon,i}^{q,k}\left(x_{EV,i}^{q,k}, \omega_{EV,i}^{q,k}\right) - C_{EV,i}^{q,k}\left(x_{EV,i}^{q,k}\right) - \left(v_{EV,i}^{q} - \theta_{EV,i}^{q}\right)x_{EV,i}^{q,k} - \lambda_{r}^{k}x_{EV,i}^{q,k}\right]'_{x_{EV,i}^{q,k*}(\lambda_{r}^{k})} = 0. \quad (30)$$

Suppose user $i$ receives the $r$th optimal power capacity data value $x_{EV,i}^{q,k*}(\lambda_{r}^{k})$, which is neither identical to $x_{EV,i}^{q,\min}$ nor $x_{EV,i}^{q,\max}$ from EV $q$. In such a case, user $i$ needs to verify that Equation (30) holds.

Here, $n$ values in the parameter vector $\omega_{EV,i}^{q,k} = \left[\omega_{1,i}^{q,k}, \omega_{2,i}^{q,k}, \cdots, \omega_{n,i}^{q.k}\right]$ can be obtained through $n$ iterations. After this process, if the data obtained do not satisfy the equation when substituted into Equation (30), the data are judged as abnormal values. That means, if Equation (30) is satisfied, the EV $q$ of user $i$ is normal; otherwise, the EV is considered to have been cyber-attack. Once the EVs under cyber-attack are identified, the smart meters of users should cut off the connection.

The process of identifying EVs under cyber-attack and processing power data is summarized as follows:

Step (1): User $i$ initializes the parameter set of EV $q$, i.e., $\omega_{EV,i}^{q,k} = \left[\omega_{1,i}^{q,k}, \omega_{2,i}^{q,k}, \cdots, \omega_{n,i}^{q.k}\right] = [0, 0, \cdots, 0]$;

Step (2): If user $i$ receives $n$ optimal power data not equal to $x_{EV,i}^{q,\min}$ or $x_{EV,i}^{q,\max}$ from EV $q$, then the elastic coefficient of EV $q$ needs to be calculated according to Equation (30), and $\omega_{EV,i}^{q,k}$ is updated;

Step (3): When user $i$ receives an $r$th optimal power data value from EV $q$ that is not equal to $x_{EV,i}^{q,\min}$ or $x_{EV,i}^{q,\max}$ the user verifies that Equation (30) is true. If Equation (30) is satisfied, then EV $q$ is normal, else, the EV $q$ is believed to be under cyber-attack.

## 5. Distribute RTP-DSG Algorithm

We combined the real-time price information a dual subgradient algorithm to design a distributed RTP-DSG algorithm. It consists of three parts: EPs, users, and PSC, shown in Figure 1.

According to Equations (23)–(27), we know that the PSC updates electricity prices while users and EPs calculate the optimal power demand and production, respectively.

Combining with MIP, users identify and deal with EVs under cyber-attack, and we obtain the framework of the RTP-DSG algorithm.

As illustrated in Figure 1, at the beginning of each time slot, the PSC initializes the price of electricity and informs all EPs and users about it. Using MIP, users process EVs' feedback power consumption depending on the given price, and then the attacked EVs are identified. The EPs update the power capacities according to Equation (25). Afterwards, all the users and EPs send the optimal data to the PSC, who updates the price according to Equation (27) and broadcasts it to users and EPs. Each time slot contains several iterations, which end when the price of electricity tends toward stability.

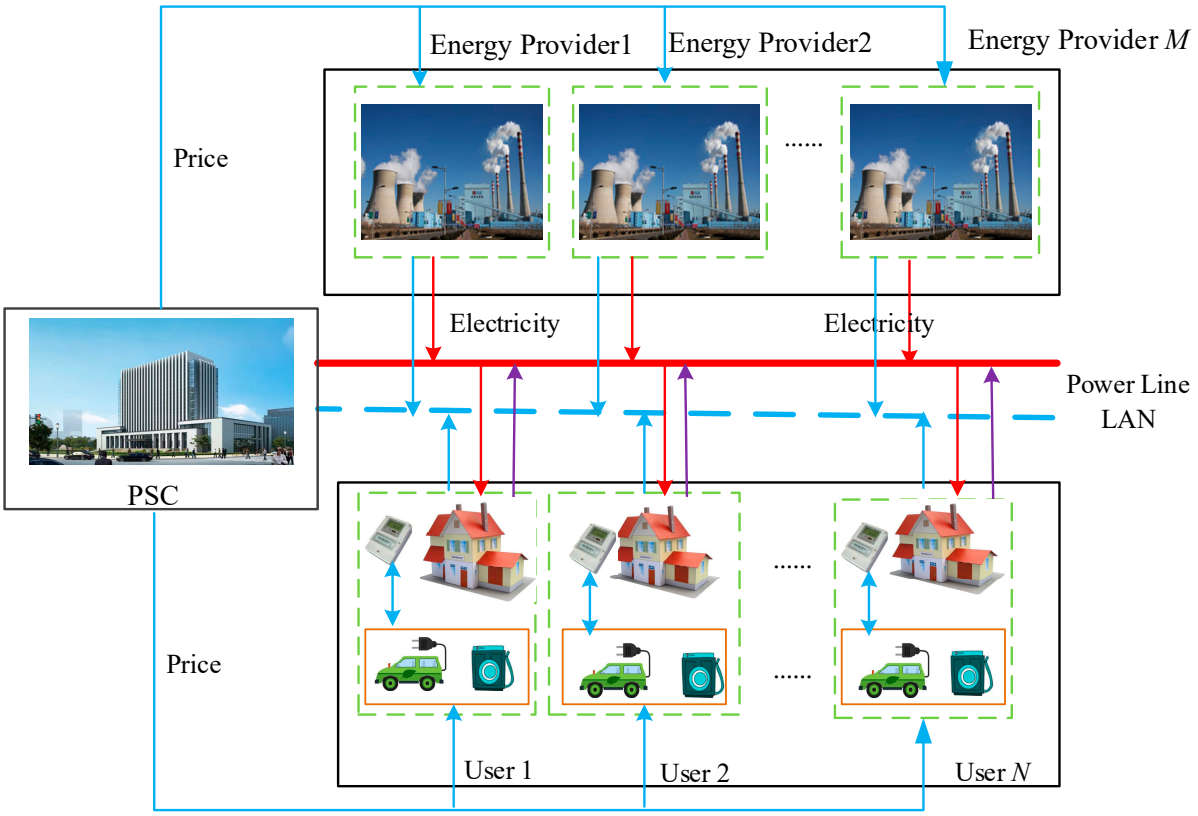



**Figure 1.** Microgrid with multiple energy providers. (Red is electricity resources, blue is price information, and purple is electricity consumption information.)

## 6. Simulation Results

This paper ran a simulation experiment several times, and the average results are given. To test the performance of the algorithm, a large number of results are presented. Unless otherwise specified, the functions and parameter settings involved are as follows:

The research considers a scenario wherein there are 5 EPs and 50 users, each equipped with 2 EVs. Among them, EVs under cyber-attack are included. We divide the time cycle of a day into 24 time slots, i.e., $\mathbb{K} = \{1, 2, \cdots, 24\}$, each of which lasts 1 h. Other relevant data for the simulations are presented in Table 2. In general, the utility function with $\omega_i^k \in [1, 3.5]$ is as follows:

$$U_{Load,i}^k(x_{Load,i}^k, \omega_{Load,i}^k) = \begin{cases} \omega_{Load,i}^k x_{Load,i}^k - \frac{1}{8}(x_{Load,i}^k)^2, & 0 \le x_{Load,i}^k \le 4\omega_{Load,i}^k, \\ 2(\omega_{Load,i}^k)^2, & x_{Load,i}^k > 4\omega_{Load,i}^k. \end{cases}$$

**Table 2.** Parameters settings.

| Parameter | Value | Parameter | Value | Parameter | Value |
|---|---|---|---|---|---|
| $y_{EP,j}^{k,\min}$ | 500 | $y_{EP,j}^{k,\max}$ | 1000 | $x_{Load,i}^{k,\min}$ | 1 |
| $x_{Load,i}^{k,\max}$ | 5 | $DOD_{i,q}^{th}$ | [0.8, 0.95] | $E_{i,q}^{\min}$ | 5 |
| $E_{i,q}^{\max}$ | [30, 50] | $a_{EV,i}^{q,k}$ | 0.2 | $b_{EV,i}^{q,k}$ | 0.1 |
| $\omega_{EV,i}^{q,k}$ | [0.4; 0.3; 0.2; 0.1] | $a_{EV,i}^{q}$ | [3; 4; 5; 6] | $[a_{EP,j}^k, b_{EP,j}^k, c_{EP,j}^k]$ | [0.05, 0.1, 0] |
| $g_{DISCH,i}^q$ | $-6$ | $g_{CH,i}^q$ | 6 | $E_{AR,i}^q$ | [5, 20] |
| $E_{TA,i}^q$ | [25, 45] | $d_1, d_2, d_3$ | 0.05 | $\varepsilon$ | 0.01 |
| $\mathbb{K}_{EV,i}^q$ | $[19, 24] \cup [1, 8]$ | $Q_{EV}^i$ | 2 | $\mathbb{K}$ | 24 |

### *6.1. Results Analysis*

Depending on the electricity price offered by the PSC, users calculate their optimal power consumption $x^k_{Load,i}(\lambda^k_t)$ in time slot $k$ after identifying and processing the power consumption of EVs under cyber-attack. Then, each user provides their total power consumption $x^k_{Load,i}(\lambda^k_t) + \sum_{q \in \mathbb{Q}^i - \mathbb{Q}^i_{CA}} x^{q,k}_{EV,i}(\lambda^k_t)$ to the PSC. The EPs also send their optimal amount of electricity information to the PSC. After collecting all information from the users and EPs, the PSC updates the price $\lambda^k_{t+1}$ based on the proposed RTP-DSG algorithm. When the algorithm satisfies the termination condition $\left|\lambda^k_{t+1} - \lambda^k_t\right| < \varepsilon$, this means the information exchange has reached the equilibrium state, then the optimal solution can be received.

The real-time electricity price of one day is shown in Figure 2. It can be seen that in the evening, the electricity price is high at the peak of power consumption, which inhibits the power demand of users. In the midnight electricity trough, the electricity price is low, encouraging users to store energy and other flexible household appliances to work. This process is helpful for the power grid to achieve the goal of peak shaving and valley filling.

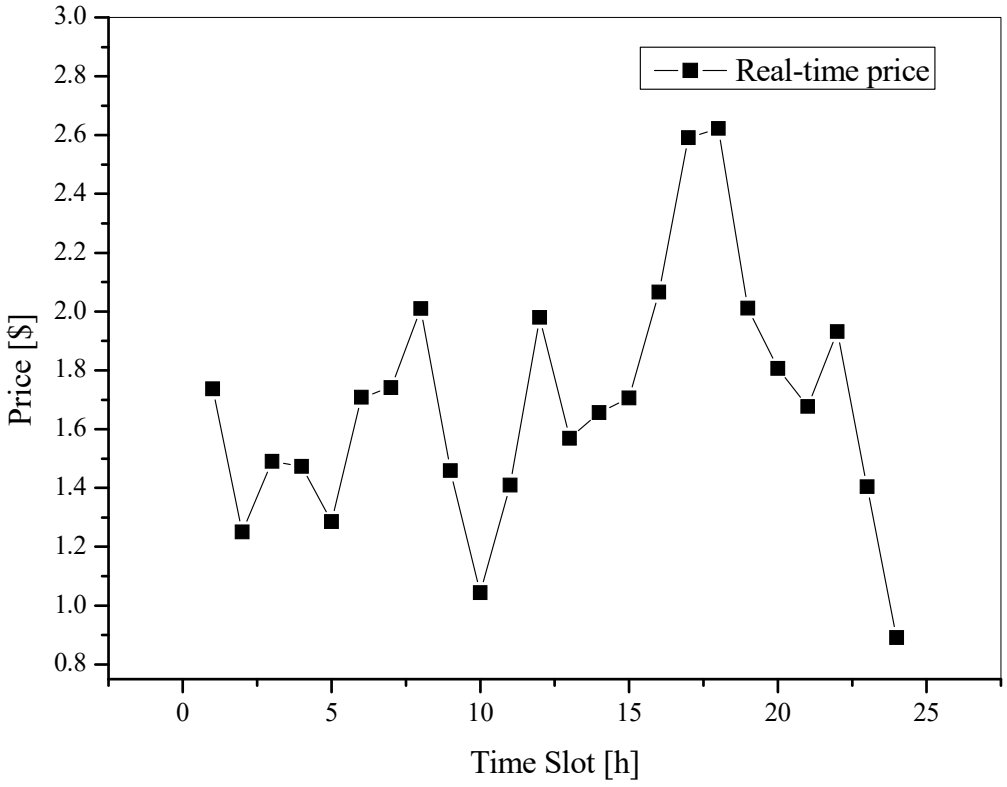



**Figure 2.** Real-time price of a day.

When the electricity price is set, the amount of electricity used by EVs is determined. We assume that the EVs leave home at eight in the morning and get home at seven in the evening. As shown in Figure 3, the optimal power consumption of two EVs at each time slot of user $i$ is obtained. At the peak of power consumption in the evening, the EVs are in the discharge state. The EVs are assessed to ensure their demand the next night. This makes full use of the mobile energy storage function of EVs.

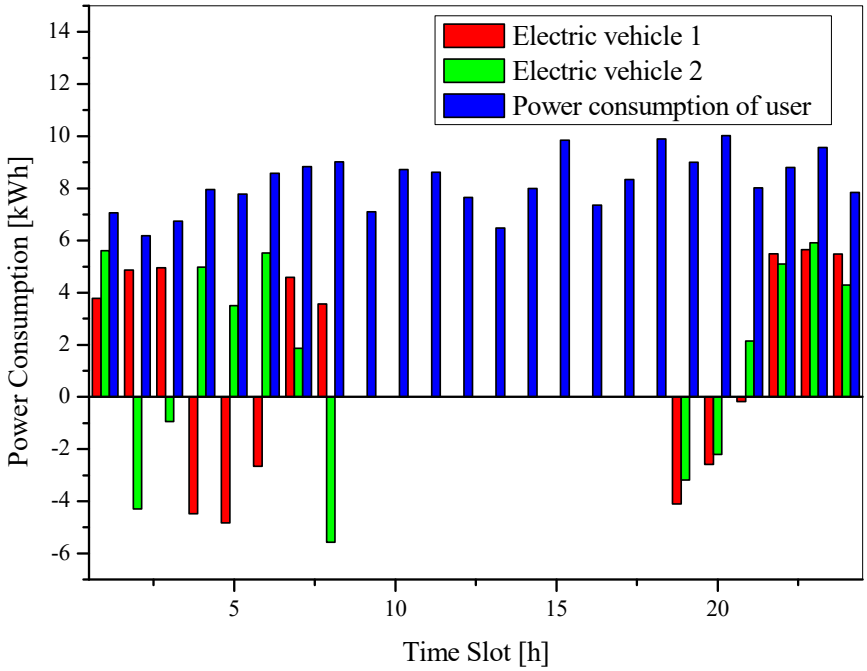



**Figure 3.** Power consumption of user at each time slot.

Figure 4 compares the total power generation and consumption at each time slot of a day. The power generation is higher than the power consumption to ensure no possibility of power failure. It can also be seen in Figure 4 that there are three power consumption peaks in a day. After the electricity price, power consumption, and generation are apparent, the social welfare value is naturally determined, as shown in Figure 5.

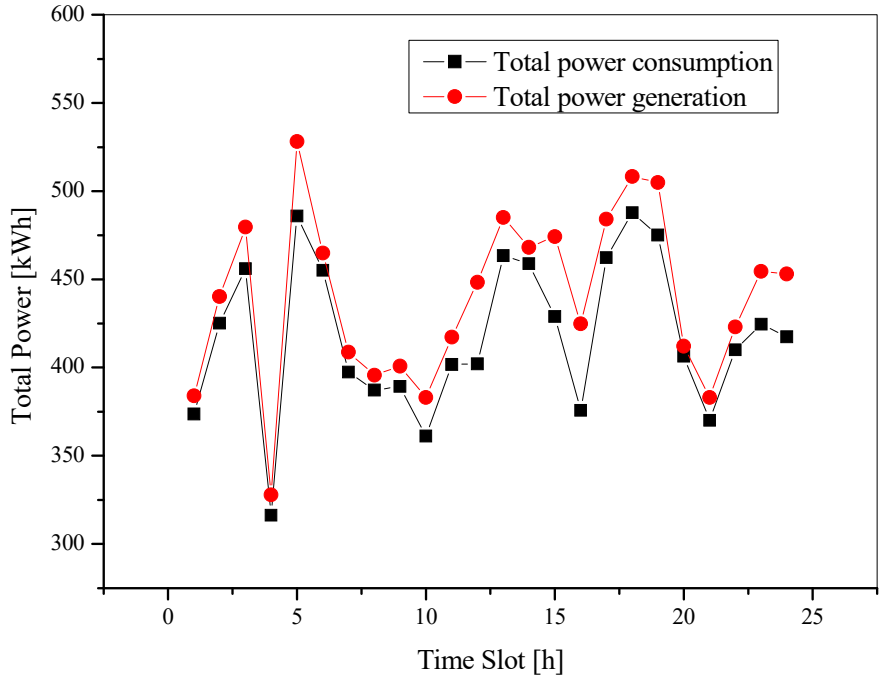



**Figure 4.** Total power consumption and generation.

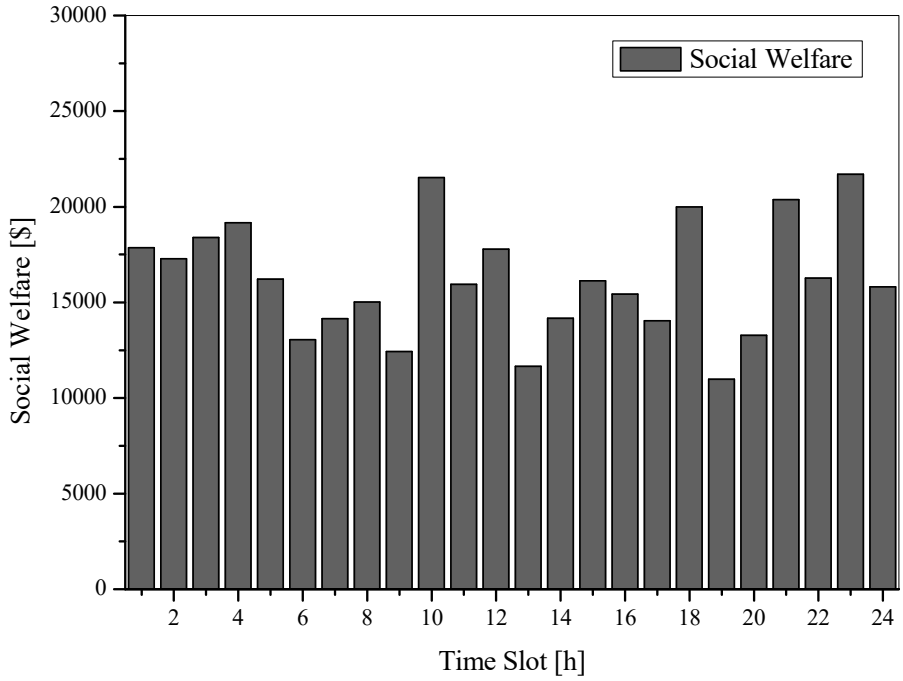



**Figure 5.** Social welfare of each time slot.

### *6.2. Comparison with Temporally Coupled Constraint and Relaxation*

By introducing Lagrange multipliers, we relax a temporally coupled constraint in P2. This operation dramatically improves the operation efficiency of the algorithm. See Figure 6 for details. The convergence speed of the algorithm is fast in both decoupled model and coupled model cases. However, the algorithm proposed in this paper can obtain more excellent social welfare value. In order to obtain a more comprehensive understanding of the social welfare obtained under the two cases, Figure 7 compares the social welfare in two cases to more intuitively show the effect of the algorithm. Our proposed algorithm is closer to the optimal solution of the model.

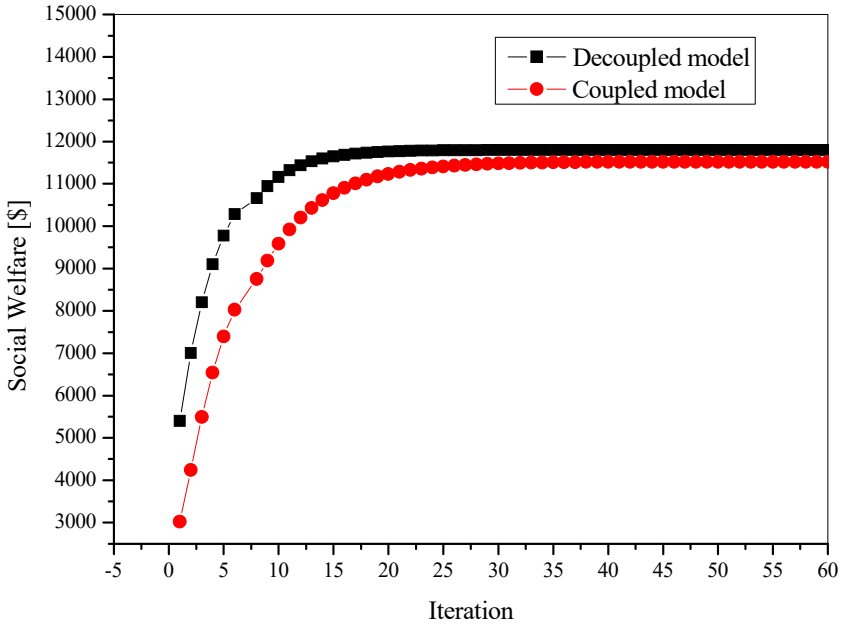



**Figure 6.** Comparison of the convergences of the models.

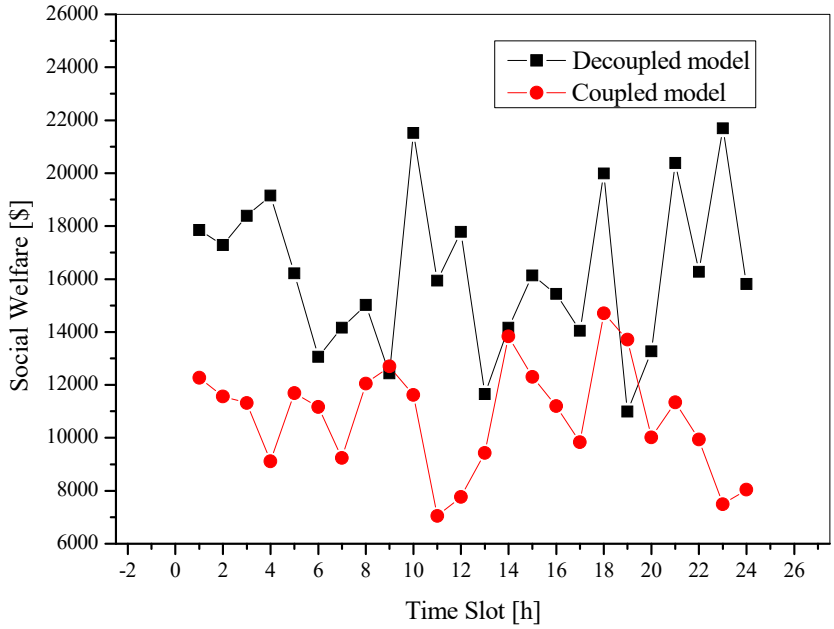



**Figure 7.** Comparison of the social welfare of two cases.

### *6.3. Contrast Reflects the Role of MIP*

The scenario we considered contains EVs under cyber-attack. If the unstable factors are not found out in time, this causes serious consequences. Next, we discuss it in two cases. In one situation, the EVs attacked by the network are not identified, leading to two consequences: one is that the optimal total power consumption (OTPC) of the users exceeds the actual power consumption (Unidentified-1), and the other is that the OTPC of the users is lower than the actual power consumption (Unidentified-2). Comparisons of convergence of electricity prices and social welfare values in cases Identified, Unidentified-1, and Unidentified-2 are shown in Figures 8 and 9, respectively. The Unidentified-1 case results in a higher electricity price than the actual value. On the EP side, this leads to excess power production and waste of power. Users need to pay more for using the same amount of power. The loss of benefits for users and EPs results in the reduction of social welfare value. Conversely, in the Unidentified-2 case, the price decreases, also hurting EPs and users. Similarly, the value of social welfare falls.

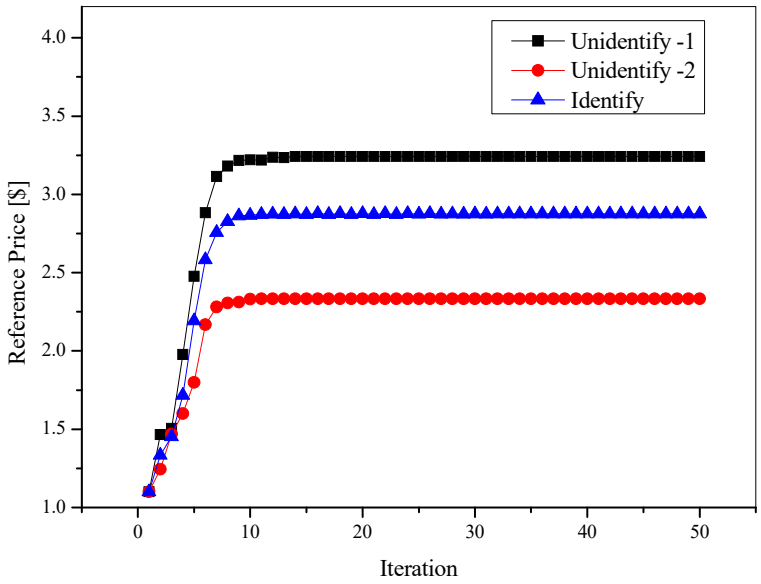



**Figure 8.** Comparison of price with Identify case and Unidentified cases.

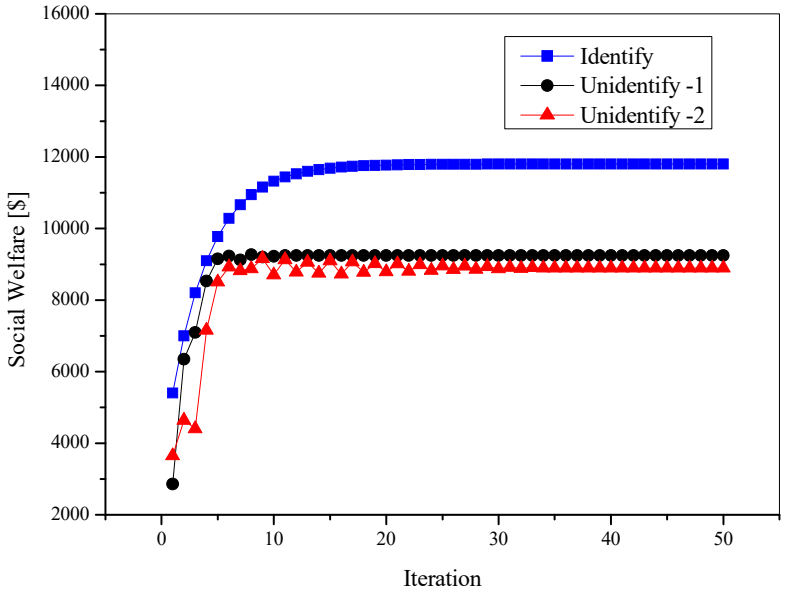



**Figure 9.** Comparison of social welfare with Identify case and Unidentified cases.

## 7. Conclusions

In this paper, an energy system with EVs under cyber-attack is considered. We construct a social welfare maximization model to make full use of the bi-directional influence between EPs and users to ensure the interests of both supply and demand. In order to reflect the utility of V2G systems, we introduce a piecewise linear function with general characteristics. This function is further smoothed to make the social welfare maximization model a convex optimization problem. Furthermore, through introducing Lagrange multipliers, we relax the time constraint condition. This guarantees that the multi-time slots social welfare model can solved separately at each time slot. The duality method is used to divide the problem into user and EP sub-problems, while protecting users' privacy. In addition, the MIP method for EVs under cyber-attack has been developed to improve the safe and stable operation of the smart grid. Through the exchange of information, the MIP identifies the EVs that have been cyber-attacked and disconnects them from the grid.

Solving the model, we obtain the RTP strategy and optimal production and demand power. The results show that the RTP can effectively realize peak cutting and valley filling. The efficiency of the solution method given in this paper is verified by comparing the time-coupling constraints and relaxation. The algorithm proposed in this paper not only converges fast but is also closer to the real optimal solution. If the EVs under cyber-attack are not identified, the utility of users is affected and the total social welfare is reduced. Finally, simulation results show that MIP can effectively screen out cyber-attacked EVs.

**Author Contributions:** Methodology, H.Z. and Z.W.; Software, H.Y. and X.Z.; Validation, X.F. and X.Z.; Formal analysis, H.Y. and Z.W.; Investigation, H.Z. and H.Y.; Resources, X.F.; Writing—original draft preparation, H.Z.; Writing—review and editing, Z.W. and H.Y.; Funding acquisition, H.Z. All authors have read and agreed to the published version of the manuscript.

**Funding:** This research was funded by the Social Science Foundation Project of Jiangsu, grant number [19GLB022] and the MOE (Ministry of education in China) Project of Humanities and Social Sciences, grant number [16YJA630032]. This work is also financially supported by the open fund for the Jiangsu Smart Factory Engineering Research Center (Huaiyin Institute of Technology).

**Data Availability Statement:** The data that support the findings of this study are available from the corresponding author upon reasonable request.

**Conflicts of Interest:** The authors declare no conflict of interest.

## Nomenclature

Nomenclature

| Abbreviations | |
|---|---|
| RTP | real-time pricing |
| EP | energy provider |
| EV | electric vehicle |
| MIP | mechanisms of identification and processing |
| MG | microgrid |
| V2G | vehicle-to-grid |
| DR | demand response |
| TOU | time of use |
| PSC | power scheduling center |
| DSG | dual subgradient |

| Sets and indices | |
|---|---|
| $\mathbb{J}$ | set of energy providers |
| $\mathbb{I}$ | set of users |
| $\mathbb{K}$ | set of time slots |
| $\mathbb{Q}^i$ | set of electric vehicles of user $i$ |
| $\mathbb{Q}^i_{CA}$ | set of all the EVs under cyber-attack |
| $j$ | index for energy provider |
| $i$ | index for user |
| $k$ | index for time slot |
| $q$ | index for electric vehicle |

Parameters

| | |
|---|---|
| $x^k_{Load,i}$ | power consumption of essential appliance (except EVs) of user $i$ in time slot $k$ |
| $x^{k,\min}_{Load,i}, x^{k,\max}_{Load,i}$ | minimum and maximum power consumption of essential appliance of user $i$ in time slot $k$ |
| $\omega^k_{Load,i}$ | elastic coefficient of user $i$ in time slot $k$ |
| $y^k_{EP,j}$ | power generation capacity of EP $j$ in time slot $k$ |
| $y^{k,\min}_{EP,j}, y^{k,\max}_{EP,j}$ | minimum and maximum power generation of EP $j$ in time slot $k$ |
| $k^q_{AR,i}, k^q_{DE,i}$ | arrival time and departure time of EV $q$ |
| $E^q_{AR,i}$ | remaining energy at arrival time |
| $E^q_{TA,i}$ | target level to be met or exceeded |
| $x^{q,k}_{EV,i}$ | charging, discharging, or idle capacity of EV $q$ |
| $\mathbb{K}^q_{EV,i}$ | V2G time |
| $g^q_{DISCH,i} g^q_{CH,i}$ | maximum discharge and charge power |
| $E^{\min}_{i,q}, E^{\max}_{i,q}$ | minimum and maximum energy stored of EV $q$ |
| $\omega^{q,k}_{EV,i}$ | elasticity coefficient vector of EV $q$ |
| $DOD^{th}_{i,q}$ | ideal maximum discharge depth of EV $q$ |
| $\lambda^k$ | electricity price of time slot $k$ |
| $v^q_{EV,i}, \theta^q_{EV,i}$ | Lagrange multipliers |
| $Q^i_{EV}$ | number of electric vehicles of user $i$ |
| $\varepsilon$ | error precision |
| $d_1, d_2, d_3$ | step sizes |
| $\alpha^k_{Load,i}$ | parameter of the utility function |
| $a^k_{EP,j}, b^k_{EP,j}, c^k_{EP,j}$ | parameters of the cost function |

## References


1. Zishan, A.A.; Haji, M.M.; Ardakanian, O. Adaptive congestion control for electric vehicle charging in the smart grid. *IEEE Trans. Smart Grid* **2021**, *12*, 2439–2449. [CrossRef]
2. Srilakshmi, E.; Singh, S.P. Energy regulation of EV using MILP for optimal operation of incentive based prosumer microgrid with uncertainty modelling. *Int. J. Electr. Power Energy Syst.* **2022**, *134*, 107353. [CrossRef]
3. Fotis, G.; Vita, V.; Maris, T.I. Risks in the European transmission system and a novel restoration strategy for a power system after a major blackout. *Appl. Sci.* **2023**, *13*, 83. [CrossRef]
4. Vita, V.; Fotis, G.; Pavlatos, C. New restoration strategy in microgrids after a blackout with priority in critical loads. *Sustainability* **2023**, *15*, 1974. [CrossRef]
5. Zafeiropoulou, M.; Mentis, I.; Sijakovic, N. Forecasting transmission and distribution system flexibility needs for severe weather condition resilience and outage management. *Appl. Sci.* **2022**, *12*, 7334. [CrossRef]
6. Zhang, X.; Chan, K.W.; Li, H. Deep-learning-based probabilistic forecasting of electric vehicle charging load with a novel queuing model. *IEEE Trans. Cybern.* **2021**, *51*, 3157–3170. [CrossRef]
7. Wang, F.; Ge, X.; Li, K.; Mi, Z. Day-ahead market optimal bidding strategy and quanti-tative compensation mechanism design for load aggregator engaging demand response. In Proceedings of the IEEE/IAS 55th Industrial and Commercial Power Systems Technical Conference, Calgary, AB, Canada, 5–8 May 2019; p. 8740412. [CrossRef]
8. Dai, Y.M.; Yang, X.Y.; Leng, M.M. Forecasting the power load: A three-stage hybrid prediction model. *Technol. Forecast. Soc. Change* **2022**, *182*, 121858. [CrossRef]
9. Dai, Y.M.; Wang, Y.X.; Leng, M.M. Lowess smoothing and random forest based GRU model: A short-term photovoltaic power generation forecasting method. *Energy* **2022**, *256*, 124661. [CrossRef]
10. Zhu, H.B.; Gao, Y.; Hou, Y. Multi-time slots real-time pricing strategy with power fluctuation caused by operating continuity of smart home appliances. *Eng. Appl. Artif. Intell.* **2018**, *71*, 166–174. [CrossRef]
11. Tao, L.; Gao, Y.; Zhu, H.B. Distributed genetic real-time pricing for multiseller-multibuyer smart grid based on bilevel programming considering random fluctuation of electricity consumption. *Comput. Ind. Eng.* **2019**, *135*, 359–367. [CrossRef]
12. Dai, Y.M.; Sun, X.L.; Qi, Y. A real-time personalized consumption-based pricing scheme for the consumptions of traditional and renewable energies. *Renew. Energy* **2021**, *180*, 452–466. [CrossRef]
13. Zhang, L.; Gao, Y.; Zhu, H.B. Bi-level stochastic real-time pricing model in multi-energy generation system: A reinforcement learning approach. *Energy* **2022**, *239*, 121926. [CrossRef]
14. Gao, J.W.; Yang, Y.; Ma, Z.Y. GGlueVaR-based participation of electric vehicles in automatic demand response for two-stage scheduling. *Int. J. Energy Res.* **2021**, *45*, 1128–1141. [CrossRef]
15. Mao, T.; Lau, W.H.; Chong, S. A regulation policy of EV discharging price for demand scheduling. *IEEE Trans. Power Syst.* **2018**, *33*, 1275–1288. [CrossRef]
16. Zhou, Z.; Wang, B.C.; Guo, Y.F. Blockchain and computational intelligence inspired incentive-compatible demand response in internet of electric vehicles. *IEEE Trans. Emerg. Top. Comput. Intell.* **2019**, *3*, 205–216. [CrossRef]
17. Yu, R.; Zhong, W.; Xie, S. Balancing power demand through EV mobility in vehicle-to-grid mobile energy networks. *IEEE Trans. Ind. Inform.* **2016**, *12*, 79–90. [CrossRef]
18. Sharma, S.; Jain, P. Risk-verse integrated demand response and dynamic G2V charge scheduling of an electric vehicle aggregator to support grid stability. *Int. Trans. Electr. Energy Syst.* **2021**, *31*, e12867. [CrossRef]
19. Zheng, Y.; Yu, H.; Shao, Z. Day-ahead bidding strategy for electric vehicle aggregator enabling multiple agent modes in uncertain electricity markets. *Appl. Energy* **2020**, *280*, 115977. [CrossRef]
20. Cao, Y.; Tang, S.; Li, C. An optimized EV charging model considering TOU price and SOC curve. *IEEE Trans. Smart Grid* **2012**, *3*, 388–393. [CrossRef]
21. Chang, T.H.; Alizadeh, M.; Scaglione, A. Real-time power balancing via decentralized coordinated home energy scheduling. *IEEE Trans. Smart Grid* **2013**, *4*, 1490–1504. [CrossRef]
22. Ding, T.; Qu, M.; Amjady, N. Tracking equilibrium point under real-time price-based residential demand response. *IEEE Trans. Smart Grid* **2020**, *12*, 2736–2740. [CrossRef]
23. Mohsenian-Rad, A.H.; Wong, V.W.S.; Jatskevich, J. Autonomous demand-side management based on game-theoretic energy consumption scheduling for the future smart grid. *IEEE Trans. Smart Grid* **2010**, *1*, 320–331. [CrossRef]
24. Samadi, P.; Mohsenian-Rad, A.H.; Schober, R. Optimal real-time pricing algorithm based on utility maximization for smart grid. In Proceedings of the 2010 First IEEE International Conference on Smart Grid Communications, Gaithersburg, MD, USA, 4–6 October 2010; pp. 415–420. [CrossRef]
25. Samadi, P.; Mohsenian-Rad, A.H.; Schober, R. Advanced demand side management for the future smart grid using mechanism design. *IEEE Trans. Smart Grid* **2012**, *3*, 1170–1180. [CrossRef]
26. Zhu, H.B.; Gao, Y.; Hou, Y. Real-time pricing considering different type of smart home appliances based on Markov decision process. *Int. J. Electr. Power Energy Syst.* **2019**, *107*, 486–495. [CrossRef]
27. Tao, L.; Gao, Y. Real-time pricing for smart grid with distributed energy and storage: A noncooperative game method considering spatially and temporally coupled constraints. *Int. J. Electr. Power Energy Syst.* **2020**, *115*, 105487. [CrossRef]
28. Zoltowska, I.; Cichosz, P.; Kolodziejczyk, W. Real-time energy purchase optimization for a storage-integrated photovoltaic system by deep reinforcement learning. *Control. Eng. Pract.* **2021**, *106*, 104598. [CrossRef]

29. Chen, Q.; Wang, F.; Hodge, B.M. Dynamic price vector formation model-based automatic demand response strategy for PV-assisted EV charging stations. *IEEE Trans. Smart Grid* **2017**, *8*, 2903–2915. [CrossRef]
30. Ren, H.; Zhang, A.; Wang, F. Optimal scheduling of an EV aggregator for demand response considering triple level benefits of three-parties. *Int. J. Electr. Power Energy Syst.* **2021**, *125*, 106447. [CrossRef]
31. Wang, B.; Dehghanian, P.; Wang, S. Electrical safety considerations in large-scale Electric vehicle charging stations. *IEEE Trans. Ind. Appl.* **2019**, *55*, 6603–6612. [CrossRef]
32. Cui, H.; Dong, X.; Deng, H. Cyber attack detection process in sensor of DC micro-grids under electric vehicle based on Hilbert–Huang transform and deep learning. *IEEE Sens. J.* **2020**, *21*, 3027778. [CrossRef]
33. Zhang, Y.Y.; Shang, J.; Chen, X. A self-learning detection method of sybil attack based on LSTM for electric vehicles. *Energies* **2020**, *13*, 1382. [CrossRef]
34. Weng, S.; Li, Y.; Ding, X. Resilient distributed coordination of plug-in electric vehicles charging under cyber-attack. *Electronics* **2020**, *9*, 770. [CrossRef]
35. Gao, Y. *Nonsmooth Optimization*; Science Press: Beijing, China, 2019.
36. Bertsekas, D.P. Nonlinear Programming. In Proceedings of the Second Berkeley Symposium on Mathematical Statistics and Probability, Berkeley, CA, USA, 31 July–12 August 1950; Neyman, J., Ed.; University of California Press: Oakland, CA, USA, 1999. [CrossRef]
37. Deng, R.L.; Yang, Z.Y.; Hou, F. Distributed real-time demand response in multiseller–multibuyer smart distribution grid. *IEEE Trans. Power Syst.* **2015**, *30*, 2364–2374. [CrossRef]


**Disclaimer/Publisher's Note:** The statements, opinions and data contained in all publications are solely those of the individual author(s) and contributor(s) and not of MDPI and/or the editor(s). MDPI and/or the editor(s) disclaim responsibility for any injury to people or property resulting from any ideas, methods, instructions or products referred to in the content.